SOFT ROBOTICS
Volume 00, Number 00, 2021
© Mary Ann Liebert, Inc.
DOI: 10.1089/soro.2021.0053

SoRo
Soft Robotics

Open camera or QR reader and scan code to access this article and other resources online.

Downloaded by Harvard University Countway Library of Medicine from www.liebertpub.com at 01/11/22. For personal use only.

An Ambidextrous STarfish-Inspired Exploration and Reconnaissance Robot (The ASTER-bot)

Michael A. Bell,[i] James C. Weaver, and Robert J. Wood

Abstract

As more roboticists are turning to Nature for design inspiration, it is becoming increasingly apparent that multisystem-level investigations of biological processes can frequently lead to unexpected advances in the development of experimental research platforms. Inspired by these efforts, we present here a holistic approach to developing an autonomous starfish-inspired soft robot that embodies a number of key design, fabrication, and actuation principles. These key concepts include integrated and sequentially deployable magnetic tube feet for site-specific and reversible substrate attachment, individually addressable flexible arms, and highly efficient and self-contained fluidic engines. These individual features offer a level of synergistic motion control not previously seen in other starfish-inspired robots. For example, our bistable dome-like tube feet are capable of achieving high adhesion forces to ferrous surfaces and low removal forces. These tube feet are further integrated with a fluidic engine to drive the entire arm while maintaining the ability to accurately control the arm position with a 270° range of motion. Furthermore, the arm and fluidic engine are modular, allowing each of the five arms to be replaced in seconds or enabling the exploration of a variety of limb geometries. Through the incorporation of these different design elements, the ASTER-bot (named for its star-like body plan) is capable of locomotion on ferrous surfaces, above and below water, and on nonplanar surfaces. This article further describes the design, fabrication, and integration strategies and characterizes the energetic and locomotory performance of this pentaradial robotic prototype.

Keywords: biomimetic robots, fluidic engine, modular soft actuator, PneuNet, soft locomotion, soft manipulation

Introduction

Echinoderms represent a remarkably diverse group of marine invertebrates, which in recent years have provided inspiration for the design of many soft robots and actuators, including those incorporating reversibly adhesive tube feet,[1–3] radially symmetrical body plans,[4–6] and crawling and undulation soft actuators.[7–11]

One group of echinoderms, in particular, that has attracted the greatest attention for the development of soft robotic prototypes is the starfish (phylum Echinodermata, class Asteroidea). Found in most marine environments and able to effectively traverse a wide range of structurally complex terrains, these echinoderms typically exhibit a pentaradial body plan with long arms, each containing hundreds to thousands of hydraulically actuated millimeter-scale reversibly adhesive tube feet with coordinated movements. Robots inspired from these characteristics are highly desirable for inspection, exploration, reconnaissance, and similar autonomous and remote tasks, where strong substrate adhesion is

John A. Paulson School of Engineering and Applied Sciences, Science and Engineering Center, Allston, Massachusetts, USA.
[i]ORCID ID (https://orcid.org/0000-0002-6002-8916).

Downloaded by Harvard University Countway Library of Medicine from www.liebertpub.com at 01/11/22. For personal use only.

critical and where wheels or propellers may be impractical. More specifically, starfish-inspired robots would be ideal for inspections of ships, pipelines, underwater structures, and for work in confined spaces.

While many previous studies of starfish-inspired robots have primarily focused on the coordination of large-scale arm movements,[12,13] or understanding the aggregated movements of tube feet, we present here the culmination of several distinct enabling technologies, including robust tube foot adhesion and release mechanisms,[1] coordinated (individually addressable) arm movements,[4] and an integrated fluidic engine,[14] all in an untethered, autonomous starfish-inspired robot (as seen in Fig. 1).

Platform

The ASTER-bot described here (named for its star-like body plan) represents a holistic approach to designing an autonomous soft bioinspired robot and includes a number of key design, actuation, fabrication, and nontraditional locomotion principles. Unlike many traditional soft robots which rely on a complex network of pumps, tubes, and switches, our actuators are both fully integrated and fully modular (Fig. 2).

The individual arms can be exchanged in seconds, allowing the robot to be customized to a specific environment, as required. The bidirectional bellow actuator that controls the movement of each arm is a closed system and, as such, functions equally well in either water or air. The tube foot magnetic adhesion mechanism can be selectively controlled, permitting their step-wise engagement ranging from 0 to 10 magnets per arm (in increments of two). Although not demonstrated in the present study, the tube feet can also be configured to control fine-scale robot movement, if locomotion is the primary goal instead of adhesion.[1,15] On the whole robot scale, locomotion is achieved through the replication of sea star gaits, through a combination of selective adhesion and coordinated with arm movement.

The arms are controlled by the robot's central, rigid hub, using peristaltic pumps to drive the bidirectional bellows using waterproofed stepper motors, while a central pump and solenoid valves drive the tube feet dome actuators. The central hub contains batteries, a microcontroller, relays, and a WiFi network card for remote, autonomous, and untethered operation. The platform is optimized to allow rapid exchange of each actuator, for both prototyping purposes and mission-specific reconfigurations.

Magnetic dome actuators

The bioinspired dome actuators, replicating the adhesion seen in many echinoderm tube feet, contain a bistable buckling dome membrane with an embedded cylindrical magnet, targeting use on ferrous surfaces, which are commonly used in marine construction. Each of the incorporated $1/8'' \times 1/4''$ (3.12×6.35 mm) cylindrical N52 neodymium permanent magnets allows for high force adhesion with zero static energy to maintain adhesion. The bistable domes passively control the trajectory of the magnet retraction—the magnets are pulled off at an angle under vacuum pressure, reducing the pull-off force to just 1/3 that of the force required to release normal to the surface. As a result, these magnetic dome actuators exhibit high-force adhesion, low force release, and zero energy adhesion.[1] The energy requirements for adhesion and release are characterized in Figure 8.

The domes were fabricated in the retracted position, at a calibrated distance, such that the magnets do not have sufficient attraction force (to a ferrous surface) to overcome the dome buckling force in the unactuated state. Furthermore, a single pneumatic line connects all dome actuators on a single arm. To allow selective actuation of each pair of dome actuators, dome thicknesses were designed ranging from 0.65 mm at the distal end to 0.875 mm at the proximal end, where the relationship of dome actuation pressure was the square of the dome thickness, as seen in Figure 2.

Fluidic engine with bidirectional bellows

The fluidic engine used for the control of each arm provides a novel method of integrating low-cost electrical position control with a soft actuator. While traditional soft actuators typically rely on a series of valves, pumps, reservoirs, and pressure transducers for control, our fluidic engine, which incorporates a peristaltic pump powered by a stepper motor, eliminates the need for most of these traditional components.

The two bellow cavities in the bidirectional actuator are principally used for planar bending actuation in the clockwise and counter-clockwise directions. Fluid is pumped through a silicone tube molded *in situ* between the two bellows with the integrated peristaltic pump, achieving the desired bending angle. The bidirectional bellows are highly efficient compared to alternative bidirectional actuators, with an electrical-to-position efficiency of $\sim 2\%$.[14,16]

Design

The ASTER-bot consists of four main components: (1) bidirectional bellow actuators for large-scale arm motion, (2) dome actuators driving permanent magnets for reversible and programmable adhesion, (3) an integrated fluidic engine for precise and high-efficiency flow control, and (4) the electrical hardware and software control system.

Actuators

Each arm consists of a bidirectional bellow actuator for large-scale movements[14] and exhibits a 270° (±135°) total bending range of motion. The arms each contain ten dome actuators with permanent magnets, which allow zero energy static adhesion (in contrast to the use of electromagnets).[1,4] The arm is molded as a single piece, integrating a peristaltic pump cap, tubing, metal support mesh, magnets, and fluidic channels as shown in Figure 2.

On each arm, the paired sets of dome actuators exhibit a graded dome thickness to control the order of deployment, allowing for pressure-controlled sequential actuation from 20 to 60 kPa within each arm, as depicted in Figure 2. All of the dome actuators are connected to a single fluidic channel through external tubing and barbed fittings. The magnets located within each dome actuator are molded in the retracted position and, upon actuation, protrude slightly from the bottom surface of the actuator as seen in Figure 2. By molding in the retracted position, the domes are slightly biased to the retracted state, reducing the vacuum pressure needed to remove them from a ferrous surface.

The integration of the dome actuators into the bidirectional bellow was a particularly challenging endeavor due to the

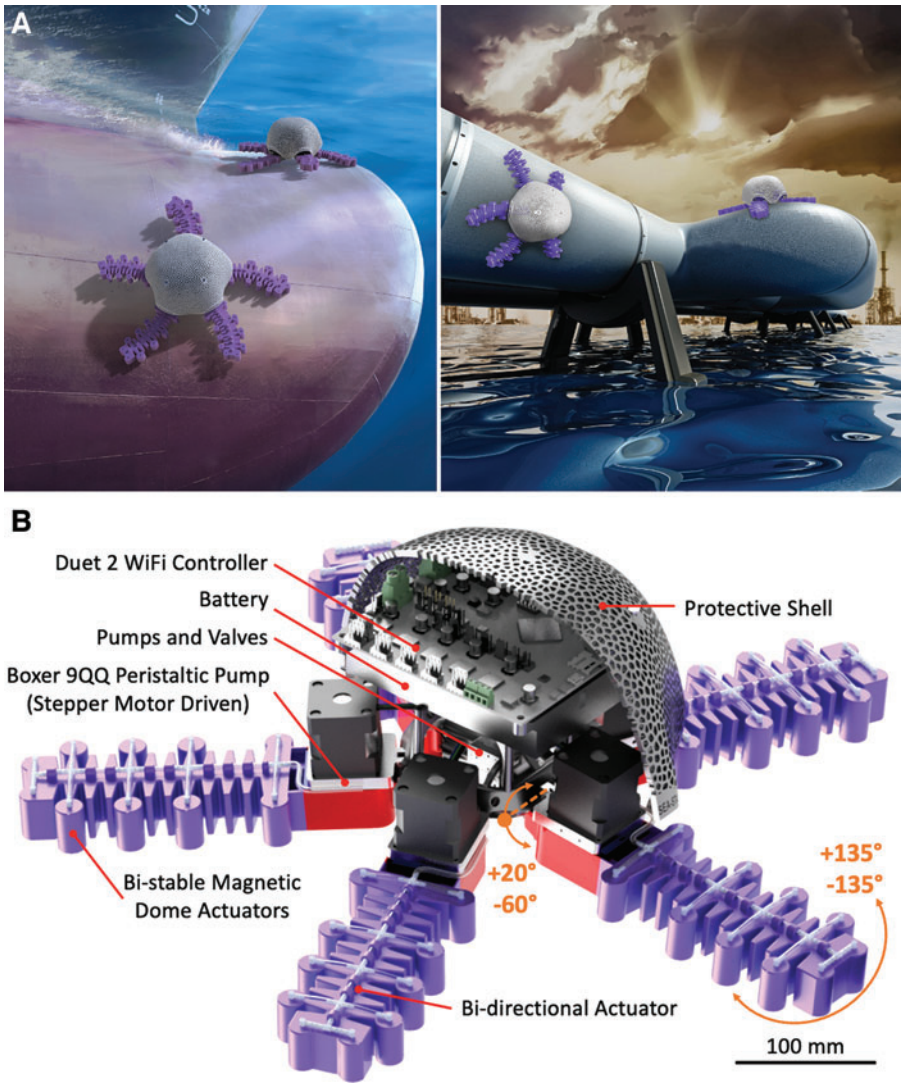

FIG. 1. Proposed applications and design elements of the ASTER-bot: **(A)** Artist's rendering of our starfish-inspired robot performing inspection tasks on boat hulls and oil pipelines. **(B)** Cross-section of the robot, 470 mm diameter × 140 mm tall, showing relevant components. Color images are available online.

intricate features of the domes relative to the coarse features of the arm. While the domes should ideally be located down the neutral axis of the bellow, all prototypes in this configuration required greater neutral axes width and thus reduced the bending performance of the bidirectional bellows. Other prototypes explored the use of individually fabricated dome actuators attached to the bellow tips, but the added bulk due to the fastening system increased weight by ∼25%.

By positioning the permanent magnets behind a 0.09 mm-thick wire mesh (RadioScreen; Less EMF, Latham, NY), the domes are theoretically each capable of achieving 3.2 N of normal pull-off force, requiring a minimum of only 10 magnets to support the weight of the entire robot (a detailed discussion of these adhesion studies is found in Adhesion section).

In the final arm design, the domes were molded as a single piece to six of the bellow tips with a spacing to ensure that the dome actuators were not the limiting geometry at a full 135° bend. With two additional domes at the arm tip and two adjacent to the peristaltic pump, each arm contained a total of 10 dome actuators. The domes were connected together with barbed fittings and tubes positioned down the top of the neutral axis. While it was possible to create an internal channel to connect all of the dome actuators without having the external tubing and fittings, the added complexity on top of an already 13-piece mold was not practical. Instead, tube routing support guides were molded into the arm to neatly anchor the supply lines in place.

As shown in Figure 2C, and Figure 5M, a small cavity is located within each of the dome actuators. This design allows a small 3/32″ (2.4 mm) barbed fitting to be inserted but requires a two-step molding process. The first molding operation creates the dome with an embedded magnet, while the second adds a controlled volume of silicone to an inverted mold using gravity to keep the liquid silicone away from the molded dome, creating the desired cavity.

Fluidic system

Each bidirectional bellow is powered by a stepper motor-driven peristaltic pump (Boxer 9QQ; Boxer, Ottobeuren, Germany) in a closed hydraulic system, as shown in Figure 3A. Fluid is pumped from one bellow to the other, and through the use of a stepper motor, the need for additional valves, regulators, tanks, or sensors is eliminated. The pump produces up to 87 kPa of pressure, which is more than

Downloaded by Harvard University Countway Library of Medicine from www.liebertpub.com at 01/11/22. For personal use only.

Downloaded by Harvard University Countway Library of Medicine from www.liebertpub.com at 01/11/22. For personal use only.

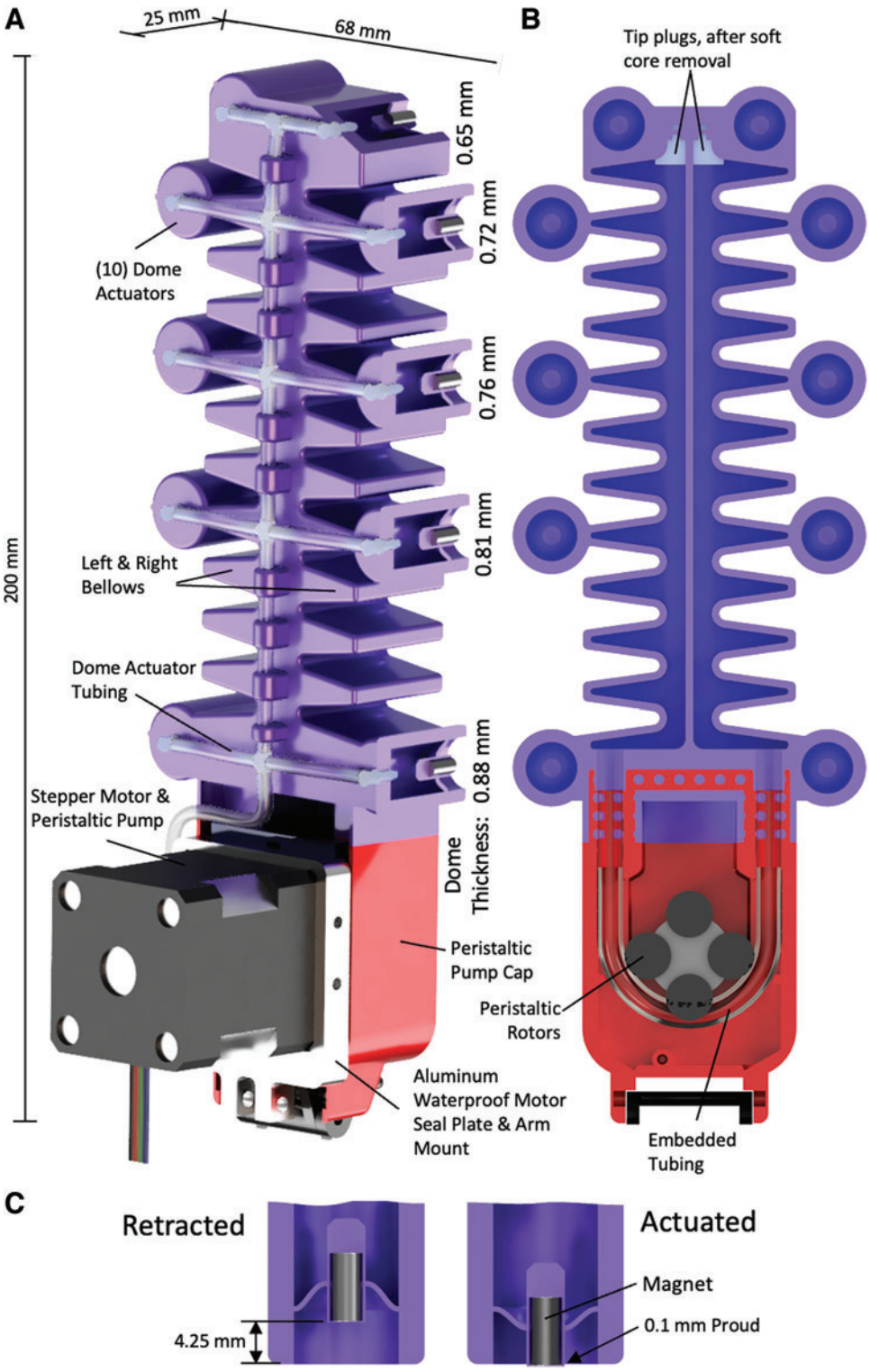

FIG. 2. Schematic representations of an integrated soft ASTER-bot arm: **(A)** Cross-section of the arm, consisting of a bidirectional bellow, integrated peristaltic pump, and 10 dome actuators with embedded magnets for adhesion. Dome actuator thickness is graded from thinnest at the distal end to thickest at the proximal end. The stepper motor is waterproofed, with an aluminum mounting plate containing shaft seals and gaskets between the stepper motor and peristaltic pump rollers. **(B)** Sectioned plan view showing the peristaltic pump mechanism, tubing, and plugs to cap the soft cores upon removal. **(C)** Dome actuators in retracted and actuated states. Color images are available online.

adequate for achieving full arm bending, and actuator position is directly mapped to stepper motor rotation when unloaded.[14] Hydraulics were chosen since peristaltic pumps do not operate well with gases, and with planned deployment in aquatic environments, the hydrostatic pressure on a gas-filled actuator could cause large deformations or bursting or exhibit undesirable changes in buoyancy.

The dome actuators are fluidically actuated, with two compact dual-diaphragm pumps (Boxer 20KD) producing upwards of 200 kPa (29 psi) of pressure and 750 mBar of vacuum. Two pumps were used in series to increase maximum vacuum pressure, which was found more effective than two in parallel (which would have increased flow rate), during removal of the dome actuators from a ferrous surface.

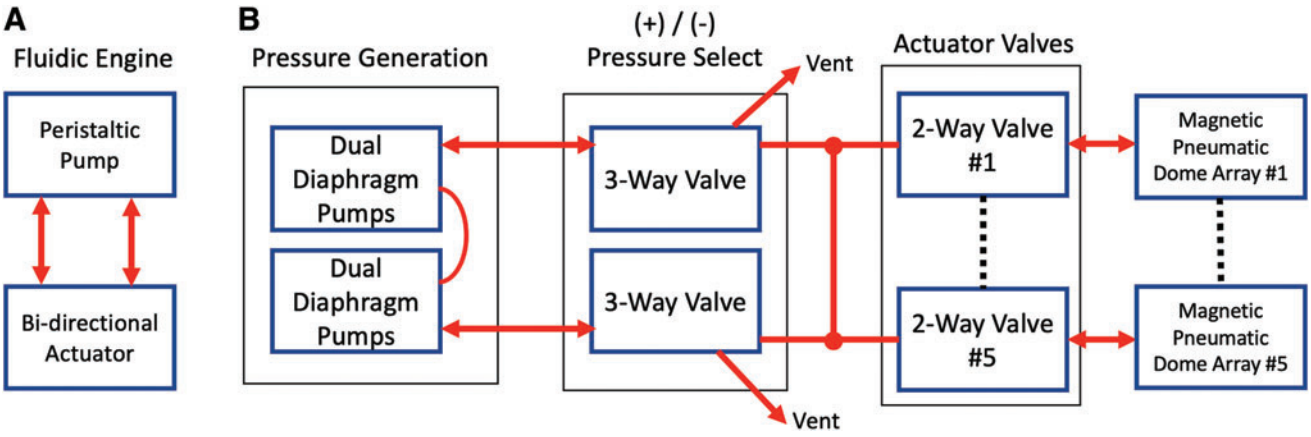

FIG. 3. Fluidic schematic for each arm of the ASTER-bot: **(A)** fluidic engine powering each bidirectional bellow; **(B)** fluidic schematic for the magnetic dome actuators. Color images are available online.

Figure 3B shows a schematic of the seven Parker X-Valves, with two of the valves used to select positive or negative pressure output from the pumps and the remaining five valves controlling arm selection. The valve and pump combination are some of the smallest available and take up a volume of just $44 \times 24 \times 55$ mm.

Simple timing of actuator inflation and deflation is sufficient to accurately control the number of inflated domes, although a pressure sensor could be used to enhance the robustness of dome actuation. The diaphragm pumps can also be replaced to match the operating environment, such as for deployment in seawater or air.

This arm design allows for high modularity: the arm docking takes only a few seconds to complete, with a barbed fitting for the domes taking an equal amount of time to exchange. This modularity thus enables the exploration of arm geometries without the need for a robot redesign. For example, significantly longer, wider, or taller arms could be fabricated with the same docking mechanism. Arms without adhesion could also be designed, or bidirectional fins could be used for a swimming-type robot.

Electrical and software system

The ASTER-bot is controlled with a Duet 2 WiFi 3D printer controller, which contains five stepper motor drivers, a WiFi module, and a number of MOSFETs. A custom six-cell (22.2v, 71 Wh) 18650-type lithium-ion battery powers the Duet, while the five fluidic engines (stepper motor-driven peristaltic pumps), two dual-diaphragm pumps, and seven valves plug directly into the Duet as seen in Figure 4. Previous studies have shown that the total efficiency of the fluidic engine is $\sim 2\%$,[14] while the energy required to actuate the magnets ranges from 0.3 to 0.57 mWh, and the energy to retract them ranges from 1.03 to 1.85 mWh, depending on the desired quantity of actuated domes (Fig. 8).

The Duet has a well-developed web interface and runs G-code, allowing for macros and scripts to simplify control of the ASTER-bot. Stepper motor position was mapped to actuator curvature, with software limits to prevent overbending. The arms were labeled as axes, X, Y, Z, U, and V. The following G-code sample commands the actuation of two magnets on the X and Y arms, moving the X arm position to

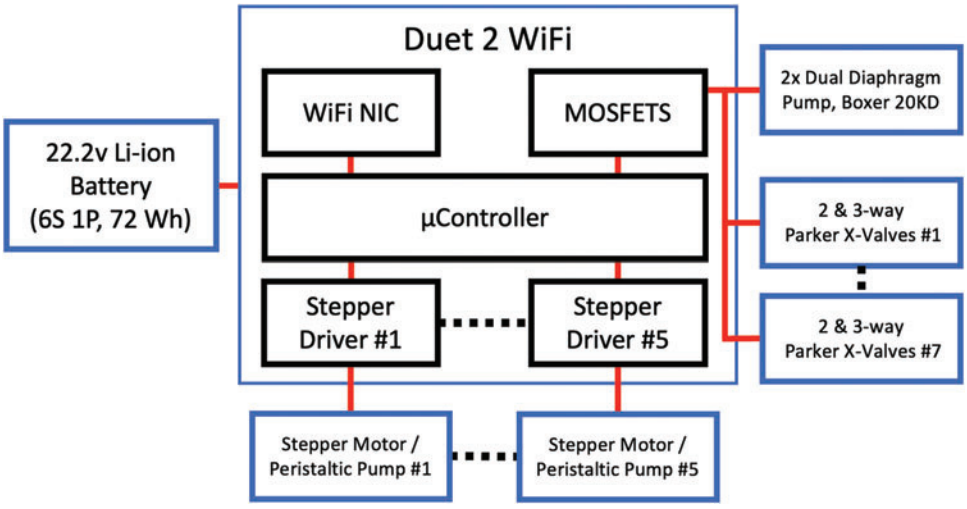

FIG. 4. The ASTER-bot electrical system, primarily consisting of a Duet 2 WiFi 3D-printer control board, capable of driving five stepper motors, a pump, and seven valves. The robot is powered by six 18650 Li-ion batteries in series. Color images are available online.

Downloaded by Harvard University Countway Library of Medicine from www.liebertpub.com at 01/11/22. For personal use only.

+90° and Y to −90°, at a speed of 1000 RPM, and then retracting two of the magnets:

M98 XA2 YA2; Magnets Actuate
G1 X90 Y-90 F1000; Bellow Movement
M98 XR2 YR2; Magnets Retract

An Untethered Pentaradial Experimental Robotics Platform: The ASTER-bot

The ASTER-bot, as diagrammed in Figure 1B, shows the platform consisting of the actuators, fluidic engine, pumps, valves, battery, and Duet 2 WiFi controller. Each arm is attached using a shoulder bolt through the custom machined aluminum waterproof motor seal plate (more clearly shown in Fig. 2), allowing an out-of-plane revolute joint of +20° to −60° to freely (passively) conform around curved surfaces such as pipes, tanks, or ship hulls. Fastening options on the motor plate allow for immobilization of this passive joint if desired. Four wires and one tube join each arm to the central hub for stepper motor power and dome actuator fluidic control. Within the central hub are the pumps and valves for the dome actuator system. The battery pack is raised to clear the stepper motors, with mounting for the Duet 2 WiFi directly above.

A porous dome-like shell provides strength and protection of the electronics, batteries, pumps, and valves while minimizing weight.[17] The porosity of the shell was designed to assist in underwater environments, preventing bubble trapping and facilitating rapid pressure equalization during submergence. The shell was designed in Rhino and Grasshopper (Robert McNeel & Associates, Seattle, WA) and produced on a Connex500 3D printer (Stratasys, Eden Prairie, MN).

Fabrication

The arms of the ASTER-bot were built upon our previously developed fabrication techniques, principally using injection molding with numerous embedded components.[1,14,15] Due to its structural complexity, our integrated actuator/pump construct presented several fabrication challenges, which resulted in a final design that consisted of a 15-piece mold and 2 injection molding operations.

As shown in Figure 5A, the bottom mold consists of 13 cores, 10 of which are used for the dome actuators. In the first step of the mold assembly process, ten metal retaining meshes and their corresponding permanent magnets were carefully inserted into each of the small cylindrical cavities (Fig. 5B). To facilitate their ease of insertion, the metal meshes were laser cut into a star shape to conform to the magnet's contours. One hundred forty millimeters of silicone tubing was then wrapped around the cap assembly (Fig. 5C).

The soft core barbed features were then inserted into the cap assembly, plugging the silicone tubing to prevent silicone ingress into the tube during molding (Fig. 5D).[18] The soft core and cap were then inserted into the bottom mold where metal rods were inserted to align and suspend the soft cores (Fig. 5E). Metal meshes were next inserted along the neutral axis to prevent the expansion of the bellow and placed around each of the dome actuator cores to prevent inflation in the radial direction (Fig. 5F). The top and bottom molds were then married, and M5 screws with flange washers were used to clamp the molds together (Fig. 5G). The completed mold was then injected with Smooth-On, Smooth-Sil 945 using a Nordson EFD Optimixer 33 static mixing nozzle (Fig. 5H).

After curing in an oven at 65°C for 30 min, the actuator was demolded, excess flash and sprue material was removed,

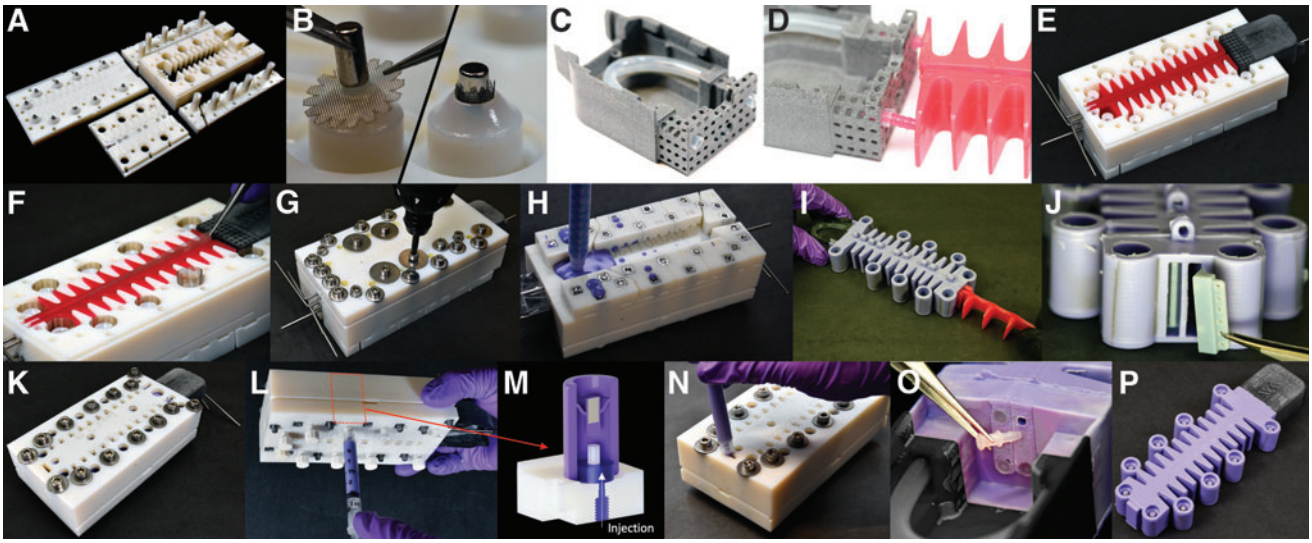

FIG. 5. Fabrication steps for a single ASTER-bot arm: **(A)** Overview of the different components of the mold; **(B)** insertion of magnets and wire mesh; **(C)** insertion of peristaltic pump tubing into the cap; **(D)** insertion of soft cores (*red*) into the tubing; **(E)** assembly of the cap and soft cores (*red*) into the mold, with rods supporting the soft cores; **(F)** insertion of inextensible mesh down the arm's neutral axis; **(G)** clamping molds with screws; **(H)** injection of silicone elastomer; **(I)** removal of soft cores (*red*); **(J)** insertion of plugs where soft cores were removed; **(K)** secondary mold operation assembled and clamped; **(L)** metered injection of silicone elastomer into the underside of the mold; **(M)** illustration of silicone injected to cap the dome actuators using gravity to keep the silicone elastomer spatially isolated from the dome membrane; **(N)** injection of silicone elastomer into the end of the mold, capping the soft core opening; **(O)** insertion of barbed plugs into the rod openings; and **(P)** the completed actuator assembly. Color images are available online.

Downloaded by Harvard University Countway Library of Medicine from www.liebertpub.com at 01/11/22. For personal use only.

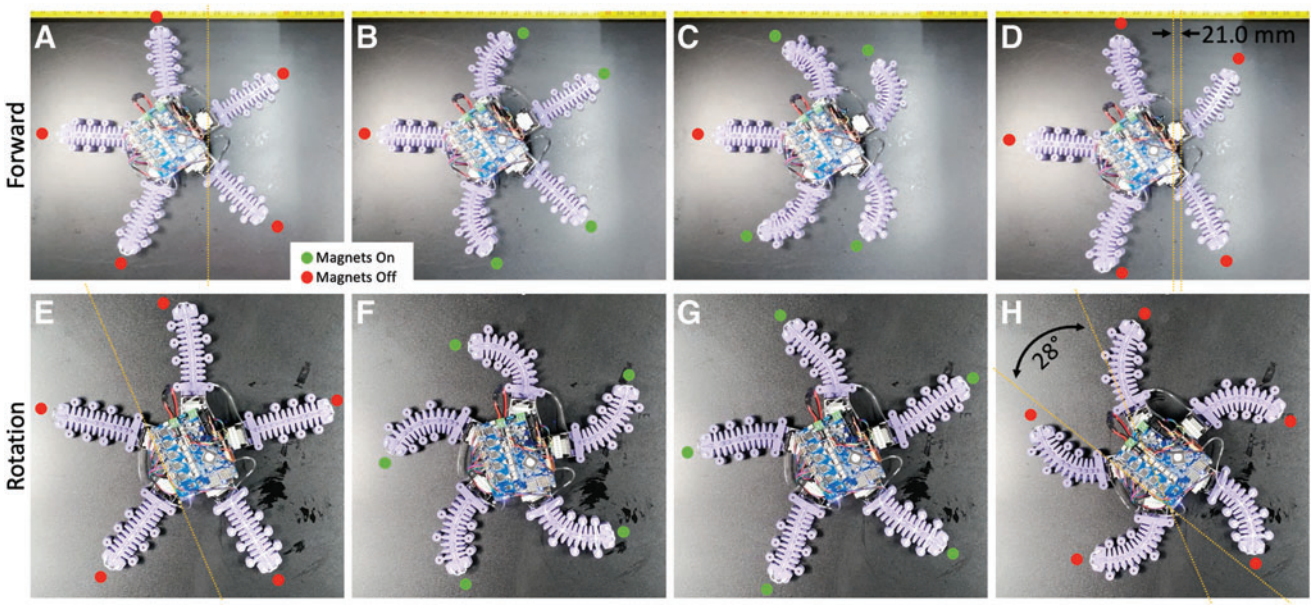

FIG. 6. Demonstration of basic gaits for forward and rotational motions in the ASTER-bot. For forward movement: **(A)** the starting state, with no magnets engaged; **(B)** the arms advance forward and the two distal magnets engage as indicated; **(C)** the actuators move backward, propelling the robot forward; **(D)** the arms then return to the neutral position and the magnets disengage, resulting in a forward movement of 21.0 mm. For rotation: **(E)** the starting state; **(F)** the arms rotate counter-clockwise and then engage the distal magnets; **(G)** the arms rotate through the neutral state; **(H)** the final position where the magnets are disengaged, resulting in a 28° rotation. Color images are available online.

and the soft cores were pulled out (Fig. 5I). The cavities for the dome actuators and soft core openings were thrice cleaned with alcohol and cotton swabs to remove any mold release residue and prepare the surface for the second molding operation. The 3D-printed inserts were then placed into the soft core openings to prevent silicone ingress into the bellow area, and small metal rods were inserted behind them to wedge them into place (Fig. 5J). The actuator was then placed into the second mold, and the top and bottom mold were secured with fasteners (Fig. 5K). A 0.7 mL volume of

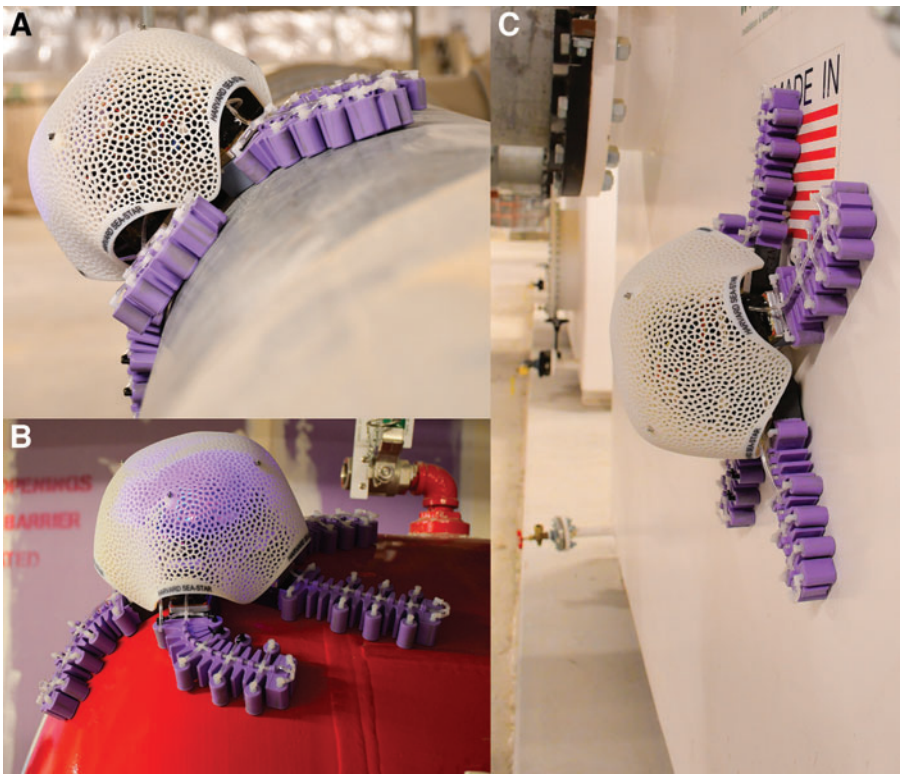

FIG. 7. Photos of the ASTER-bot adhering and conforming to the ferrous surfaces of a pipe **(A)**, fire suppression tank **(B)**, and a vertical wall **(C)**. Color images are available online.

Downloaded by Harvard University Countway Library of Medicine from www.liebertpub.com at 01/11/22. For personal use only.

Smooth-Sil 945 was then metered using an upside-down syringe into each dome actuator port through a luer-lock fitting and then quickly capped when complete to prevent the silicone from contacting the dome actuator (Fig. 5L, M). Silicone was also injected into the top port to cap the soft core opening (Fig. 5N).

The second molding step was cured at 65°C for 30 min, and the completed actuator was removed and filled with water using a syringe and barbed plugs (Fig. 5O, P).

For each arm, the entire manufacturing process took ca. 2.5 h, including mold assembly, elastomer injection, curing, and the second molding step.

Characterization

Gaits

Simple forward and rotational gaits were performed to demonstrate the system's potential ranges of motion, as depicted in Figure 6. In the forward movement sequence shown in Figure 6A–D, four arms are used to propel the robot forward (in this gait, the trailing arm does not perform useful work). The gait begins with all magnets retracted and arms in the neutral position. The top and bottom arms are then commanded to bend slightly forward as seen in Figure 6B, and then the two most distal magnets on the four arms are

Downloaded by Harvard University Countway Library of Medicine from www.liebertpub.com at 01/11/22. For personal use only.

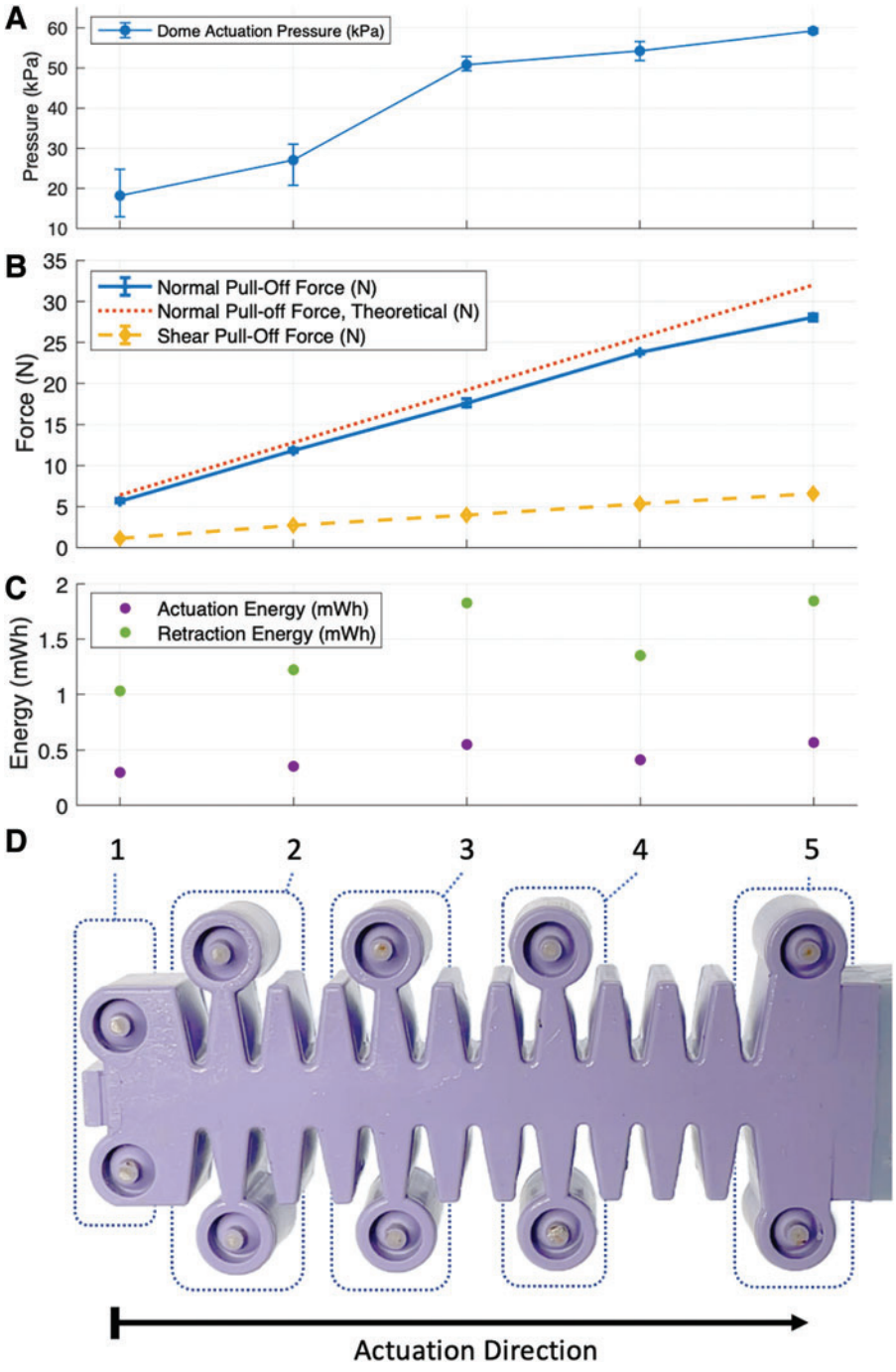

FIG. 8. Characterization of the ASTER-bot dome actuators: **(A)** pressures required to actuate each pair of domes with accompanying normal and shear pull-off forces; **(B)** actuation and retraction energy required for each pair of domes; **(C)** location of each dome pair and actuation direction sequence, from distal (1) to proximal (5); and **(D)** actuator diagram showing actuation direction. Color images are available online.

actuated. The four arms are then commanded to bend backwards as seen in Figure 6C, which cause each arm to pivot around the anchored magnets and propel the robot forward. The magnets are then retracted, and the arms are returned to the neutral position as seen in Figure 6D. The robot moves 21.0 mm with each sequence, with a cost of transport of 576. Using this arm actuation sequence also allows for instantaneous changes in direction since any arm can adopt the trailing arm's stationary role.

In the rotational sequence shown in Figure 6E–H, all arms first move counter-clockwise from the starting state and then engage the two distal magnets as seen in Figure 6E and F. Once attached, all arms move clockwise until the maximum limit is reached and the magnets are disengaged (Fig. 6G, H). For each of the above sequence of events, the robot rotates 28°.

Movement on vertical or curved surfaces (Fig. 7) requires a more complex gait movement, since the arms must anchor the robot, as well as propel it. In the case of the pipe and tank shown in Figure 7A and B, at least three arms are used to anchor the robot, while the others rotate and move into position, then fully anchor, with all ten arm magnets engaged. This process is repeated until all arms are in position, such as in Figure 6B for forward movement or 6F for rotational movement. To maintain adequate adhesion during the final movement sequence, the magnets are retracted until the only four distal magnets remain engaged on all of the arms (except the trailing arm during a forward movement cycle, in which two distal magnets are kept engaged, to keep the arm from releasing from a curved surface). The final movement sequence is then performed, which while still effective results in less forward or rotational movement due to the added adhesion of the magnets.

Movement on a vertical surface, such as in Figure 7C, is similar to movement on curved pipes and tanks but requires six distal magnets to be engaged, further reducing the incremental extent of forward or rotational movements. No more than one arm can be fully disengaged at any time or the robot may be at risk of sliding down the vertical surface (the shear force of the magnets is less than the normal pull-off force, and as such, holding onto a vertical surface is the most challenging). While transitioning from horizontal to vertical substrates without a surface radius of curvature of 30 cm or greater is not possible since the arms have only a passive out-of-plane movement, this could in theory be partially mitigated underwater through the addition of a buoyancy control mechanism beneath the central porous dome-like shell to achieve additional ranges of motion.

Adhesion

Since each pair of dome actuators exhibits a sequential reduction in wall thickness from the most proximal to the most distal, when pressurized, the distal-most pair actuates first, and the domes actuate sequentially until the finally proximal-most pair is actuated. Each pair of domes takes 200–400 ms to actuate (3 s for a full arm), with retraction taking ~800 ms per pair (8 s for a full arm). Full actuation is useful for maximum adhesion to a surface, while only actuating the distal actuators allows for useful gait movements while pivoting. Figure 8 details the pressure and force results for each pair of dome actuators with accompanying images of the domes in their actuated state. Normal and shear pull-off forces are also shown for each actuated dome pair.

Table 1. Mechanical Property Metrics (in Air) for the ASTER-bot

Robot weight (with shell)	*2.99 kg*
Arm weight (no pump)	190 g
Arm weight (with pump)	407 g
Shell weight	189 g
Theoretical pull-off force	160 N
Measured pull-off force	139 N
Shear force	27.9 N

The permanent neodymium magnets in the dome actuators exhibit a theoretical pull-off force of 3.2 N each, allowing for a total of 32 N of adhesion per arm, and for the full robot, 160 N. In reasonable agreement with these theoretical values, experimental results show 139 N of total required pull-off force for a lightly textured, powder-coated steel sheet. With the total robot weighing ca. three kilograms, an adhesion factor of safety of nearly 5× is achieved (Table 1). This extreme redundancy in the required versus available adhesion strength opens several exciting options for exploring application-specific gates in our ASTER-bot.

For example, with minimal arm contact, such as would occur with only two or three arms anchoring, the other arms can quickly reposition as part of the gait cycle. This redundant design also allows for partial clamping of arms, where the distal one or two pairs of magnets on all arms could hold the robot in place, while all of the bellows synchronously bend—creating an in-place rotation (Fig. 6E–H).

Conclusions and Future Directions

Our starfish-inspired ASTER-bot combines several unique technologies into an untethered and highly modular soft robotics research platform. The ASTER-bot contains a set of novel fluidic engines, driving five bidirectional bellows, each capable of a 270° range of rotation, and incorporates 10 fluidic-actuated permanent magnets (per arm), which permit zero-energy static adhesion to a variety of geometrically diverse ferrous surfaces.

The efficient and independently addressable fluidic engines that drive each of the five arms also offer the unique opportunity to develop application- or substrate-specific gaits by modulating frictional contact with the ground, limb actuation sequences, and the syncing of tube feet into limb movement for coordinated locomotion.[3,12,13] Toward these efforts, additional investigations into environment- or substrate-specificity in a wide range of starfish species could lead to the development of a set of design rules that identify correlations between arm aspect ratio and habitat topographical complexity or cross-sectional arm geometries that are adapted to specific ambient water current velocities.[19]

Beyond task- or application-specific gait optimization, the highly modular design of the ASTER-bot would allow for additional investigations into the effects of arm geometry on object grasping and manipulation. Because of the large safety factor for substrate adhesion permitted by the numerous high-strength neodymium magnets on each arm, future ASTER-bot iterations could incorporate multiple arm geometries into a single prototype, for the creation of hybrid body plans that incorporate different appendage form factors that are

Downloaded by Harvard University Countway Library of Medicine from www.liebertpub.com at 01/11/22. For personal use only.

structurally optimized for achieving specific tasks such as substrate anchoring or object manipulation. In terms of system robustness, due to the highly modular and fully self-contained nature of the fluidic engines, the actuators can be quickly replaced due to changing mission parameters or if damaged during routine operation.

On the material optimization side of things, the highly versatile manufacturing methods used to fabricate the arms could also be adapted to provide several options for future soft robot development, including the incorporation of multiple types of material inserts, elastomers with a diverse range of moduli, and complex geometries with wall thicknesses down to 0.65 mm.

With some modifications, the ASTER-bot could also be used for deep-sea applications, such as routine monitoring of underwater structures, ship hulls, oil platforms, underwater pipelines, or be outfitted to perform cleaning and manipulation tasks. To perform such tasks, the stepper motors, which are currently water-proofed for shallow depths through an epoxy coating and rotary shaft seals, would need to be filled with transformer oil to eliminate any air. The electronics, including the controller and batteries, would also need to be cast in epoxy to prevent water exposure. Finally, the magnetic dome actuators would need to be actuated with a hydraulic pump using sea water, rather than with their current pneumatic configuration.

Beyond these more robust water-proofing design changes, the robot could also be engineered to exhibit a near-neutral buoyancy, significantly improving its underwater adhesion safety factor. Autonomous navigation and inspection would be ideal for underwater use, since untethered remote control at depth is a challenge since WiFi and high frequency radio signals cannot travel any substantial distance through water. As such, low frequency protocols would have to be used for basic robotic operations, such as commanding the robot to return to its origin.

As demonstrated here, our ASTER-bot and the fabrication technologies that were used to construct it thus offer a highly modular and adaptable soft robotics platform that can be used for both research and educational applications aimed at identifying structure–function relationships in environment- and task-specific soft fluidic actuators.

Acknowledgments

Special thanks to Lara Tomholt (Harvard Graduate School of Design) and Juan Carlos Noguera (Maryland Institute College of Art) for robot shell design and artist's renderings.

Author Disclosure Statement

No competing financial interests exist.

Funding Information

The authors gratefully acknowledge support from the Office of Naval Research (Award No. N00014-17-1-2063).

References

1. Bell M, Pestovski I, Scott W, *et al.* Echinoderm-inspired tube feet for robust robot locomotion and adhesion. IEEE Robot Autom Lett 2018;3:2222–2228.
2. Sadeghi A, Beccai L, Mazzolai B. Design and development of innovative adhesive suckers inspired by the tube feet of sea urchins. In: Proceedings of the IEEE RAS and EMBS International Conference on Biomedical Robotics and Biomechatronics, (Rome, Italy). New York, USA: IEEE, 2012, pp. 617–622.
3. Heydari S, Johnson A, Ellers O, *et al.* Sea star inspired crawling and bouncing. J R Soc Interface 2020;17:20190700.
4. Paschal T, Bell M, Sperry J, *et al.* Design, fabrication, and characterization of an untethered amphibious sea urchin-inspired robot. IEEE Robot Autom Lett 2019;4:3348–3354.
5. Mao S, Dong E, Jin H, *et al.* Gait study and pattern generation of a starfish-like soft robot with flexible rays actuated by SMAs. J Bionic Eng 2014;11:9.
6. Calisti M, Arienti A, Renda F, *et al.* Design and development of a soft robot with crawling and grasping capabilities. In: 2012 IEEE International Conference on Robotics and Automation. New York, USA: IEEE, 2012, pp. 4950–4955.
7. Shepherd RF, Ilievski F, Choi W, *et al.* Multigait soft robot. Proc Natl Acad Sci U S A 2011;108:20400–20403.
8. Mao S, Dong E, Zhang S, *et al.* A new soft bionic starfish robot with multi-gaits. In: Proceedings of IEEE/ASME International Conference on Advanced Intelligent Mechatronics, (Wollongong, NSW, Australia). New York, USA: IEEE, 2013, pp. 1312–1317.
9. Umedachi T, Vikas V, Trimmer BA. Softworms: the design and control of non-pneumatic, 3D-printed, deformable robots. Bioinspir Biomim 2016;11:025001.
10. Tolley MT, Shepherd RF, Mosadegh B, *et al.* A resilient, untethered soft robot. Soft Robot 2014;1:213–223.
11. Rus D, Tolley MT. Design, fabrication and control of soft robots, Nature 2015;521:467–475.
12. Scott WL, Paley DA. Geometric gait design for a starfish-inspired robot with curvature-controlled soft actuators. In: Proceedings of ASME Dynamic Systems and Control Conference, (Tysons, VA, USA). New York, USA: ASME, 2017, p. V002T07A005.
13. Scott WL, Paley DA. Geometric gait design for a StarfishâĂŘInspired robot using a planar discrete elastic rod model. Adv Intell Syst 2020;2:1900186.
14. Bell MA, Gorissen B, Bertoldi K, *et al.* A modular and self-contained fluidic engine for soft actuators. Tech. Rep., 2021.
15. Bell MA, Cattani L, Gorissen B, *et al.* A soft, modular, and bi-stable dome actuator for programmable multi-modal locomotion. In: 2020 IEEE/RSJ International Conference on Intelligent Robots and Systems (IROS), 2020, pp. 6529–6535.
16. Marchese AD, Katzschmann RK, Rus D. A recipe for soft fluidic elastomer robots. Soft Robot 2015;2:7–25.
17. Tomholt L, Friesen LJ, Berdichevsky D, *et al.* The structural origins of brittle star arm kinematics: an integrated tomographic, additive manufacturing, and parametric modeling-based approach. J Struct Biol 2020;211:7.
18. Galloway KC, Becker KP, Phillips B, *et al.* Soft robotic grippers for biological sampling on deep reefs. Soft Robot 2016;3:23–33.
19. Hayne KJ, Palmer AR. Intertidal sea stars (Pisaster ochraceus) alter body shape in response to wave action. J Exp Biol 2013;216:1717–1725.

Address correspondence to:
Michael A. Bell
John A. Paulson School of Engineering and Applied Sciences
Science and Engineering Center
150 Western Avenue
Allston, MA 02134
USA

E-mail: bell@seas.harvard.edu

Downloaded by Harvard University Countway Library of Medicine from www.liebertpub.com at 01/11/22. For personal use only.